Science of the Total Environment 661 (2019) 10–17

Contents lists available at ScienceDirect

Science of the Total Environment

journal homepage: www.elsevier.com/locate/scitotenv

Short-term prediction of extremely hot days in summer due to climate change and ENSO and related attributable mortality

Chu-Chih Chen [a,*], Ying-Ru Wang [a], Yue-Liang L. Guo [b], Yu-Chun Wang [c], Mong-Ming Lu [d,**]

[a] Division of Biostatistics and Bioinformatics, Institute of Population Health Sciences, National Health Research Institutes, Taiwan
[b] National Institute of Environmental Health Sciences, National Health Research Institutes, Taiwan
[c] Department of Bioenvironmental Engineering, College of Engineering, Chung Yuan Christian University, Taiwan
[d] Department of Atmospheric Sciences, National Taiwan University, Taiwan

HIGHLIGHTS

- Nonlinear lagged association between ENSO and extremely hot days in summer
- Flexible estimate of nonlinear climate change trend
- Short-term prediction model for extremely hot days with high precision
- Risk map of county-specific heat-attributable mortality
- Provide a tool and guidance for health policy for imminent threat of climate change

GRAPHICAL ABSTRACT

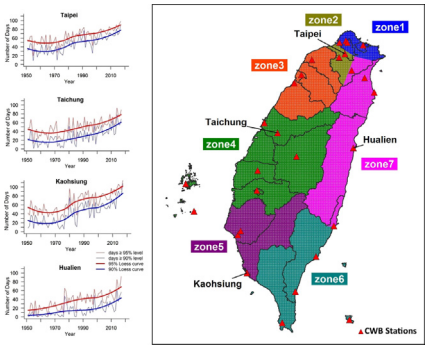

ARTICLE INFO

Article history:
Received 25 September 2018
Received in revised form 21 December 2018
Accepted 13 January 2019
Available online 15 January 2019

Editor: SCOTT SHERIDAN

Keywords:
Autocorrelation
Comparative risk assessment
Distributed-lag nonlinear model
Lag effect
Locally weighted scatter plot smoothing
State-space model

ABSTRACT

Summer days with extremely hot temperatures in Taiwan have been increasing for the past few decades, and this continuing trend is expected to worsen heat-related mortality. To mitigate the corresponding health impacts, in this study, we developed a statistical state-space model to predict the number of extremely hot days in June–September for the next year. Based on historical data from 1951 to 2017, we estimated the climate change trend after adjusting for the nonlinear lagged effect of the Niño 3.4 index. We then developed a predictive state-space model using these two primary factors and adjusting for residual autocorrelations. Validation results comparing the extremely hot days observed over 2015–2017 with predictions showed that 86% of the average prediction errors were within 4 days of the observations. To assess the health impacts, we applied the model to the projection of heat-attributable mortality (AM) in 2018 by adopting a comparative risk assessment (CRA) approach with the reference period of 2001–2010. The results showed that the Taipei metropolitan area in northern Taiwan is the most affected region with AM of 1501 deaths from all-causes, followed by Taichung in central Taiwan with 490 deaths. The prediction model and the CRA projection provide both a tool and guidance for public health administrators to address the imminent threat posed by climate change.

© 2019 Elsevier B.V. All rights reserved.

* Correspondence to: C.-C. Chen, Division of Biostatistics and Bioinformatics, Institute of Population Health Sciences, National Health Research Institutes, 35 Keyan Road, Zhunan, Miaoli 350, Taiwan.
** Correspondence to: M.-M. Lu, Department of Atmospheric Sciences, National Taiwan University, 1 Sec. 4, Roosevelt Road, Taipei 106, Taiwan.
E-mail addresses: ccchen@nhri.org.tw (C.-C. Chen), mongminglu@ntu.edu.tw (M.-M. Lu).

https://doi.org/10.1016/j.scitotenv.2019.01.168
0048-9697/© 2019 Elsevier B.V. All rights reserved.

1. Introduction

The global mean temperature has been continually rising over the past one hundred years, especially since the end of the last century. The year 2016 was the warmest year since 1880, followed by 2015 and 2017 as the second and third warmest years, respectively. The period of 2015–2016 was marked by a very strong El Niño, while 2016–2018 was influenced by a weak La Niña (NOAA, 2017). El Niño Southern Oscillation (ENSO) is the most powerful mode of climate variability that can modulate precipitation and temperature anomalies over many regions of the world (Cannon, 2015; Leung and Zhou, 2016; Ratnam et al., 2016). ENSO is known as the most important predictor in regional climate forecasts on seasonal to interannual time scales (Cannon, 2015; Chen et al., 2013; Kuo et al., 2010; Larkin and Harrison, 2005; Leung and Zhou, 2016; Peng et al., 2014; Rohini et al., 2016). It is also known to be a strong influential factor of rainfall extremes or drought (Chen et al., 2013; Kuo et al., 2010) and heat waves (Luo and Lau, 2018; Perkins, 2015).

Studies have shown that extremely high temperatures increase mortality globally (Gasparrini et al., 2015; Guo et al., 2014). For example, the 2003 heat waves in southern Europe caused nearly 15,000 deaths in France alone (Vandentorren et al., 2006). Also, the 2009 heat wave in Australia leaded to a 62% increase in mortality in Melbourne (Nitschke et al., 2011; Zuo et al., 2015). Because of global warming, it is expected that heat-related mortality will increase while cold-related mortality will decrease (Lee and Kim, 2016). In Taiwan, the relative risk of heat-related mortality increased significantly when daily mean heat indices (mean, maximum, and minimum temperature, heat index, etc.) exceeded the 95th percentile in several major cities (Lin et al., 2012; Sung et al., 2013). It is therefore of great importance to be able to make city-specific predictions of extremely hot days to provide an early warning system for increased mortality risk.

Projections of temperature-attributed mortality due to future climate change are often based on global/regional climate models (GCM/RCM) under different scenarios (Honda et al., 2014; Lee and Kim, 2016). However, great uncertainties exist in the projections among different climate models (Stephenson et al., 2012). Apart from the impacts of ENSO on extreme weather, statistical modeling to predict climate extremes based on historical observations has been shown to exhibit less uncertainty (Guttorp and Xu, 2011; Qian et al., 2015; Zhang et al., 2018). To predict hot temperature extremes in Macao, Qian et al. (2015) proposed a linear statistical model for the relationship between transformed hot days with daily maximum temperature exceeding 33 °C (HD33) and modified El Niño Modoki index (MEMI) and Atlantic multidecadal oscillation (AMO), along with other predictors. The predictability of the annual occurrences of hot days and hot nights in Macao was attributed to the interannual and interdecadal variability of the coupled ENSO-East Asian summer monsoon system. The authors suggested that the physically based statistical prediction model can be used as a downscaling method when applied to the climate projection model dataset, such as the phase 5 of the Coupled Model Intercomparison Project (CMIP5) multimodel dataset, to project the future change. Zhang et al. (2018) found spring soil temperature over Central Asia and sea surface temperature (SST) over Northwest Atlantic are good predictors for hot days in summer over the source region of ancient Silk Road. They suggested that the proposed statistical models can be applied to operational seasonal forecast. Indeed, forecasting temperature-related mortality within the next year is of more pressing importance than long-term projection for public health policy and administration.

In the present study, we propose a state-space model to predict the number of days with extreme heat in Taiwan. We then use the statistical model for the projection of heat-related attributable mortality (AM) in June–September of the next year. We establish the time-series model by assessing the lagged effects of Niño 3.4 on extreme daily temperatures in Taiwan, together with a trend estimate of climate change based on historical data from 1951 to 2017. Based on the prediction outcomes, we adopt a comparative risk assessment (CRA) approach for the projection with the reference period of 2001–2010.

2. Materials and methods

2.1. Data

We obtained hourly temperature records from 36 Taiwanese meteorological stations from the Data Bank for Atmospheric & Hydrologic Research of Taiwan Typhoon and Flood Research Institute along with the monthly Niño 3.4 index covering the 1951–2017 period. Among the 36 stations across Taiwan, 12 stations were located in mountains over 1000 m or had incomplete measurement records during the study period and were excluded from the analysis. For demographic data, we obtained yearly population size during 2010–2017 and national mortality data in 2016 from the Ministry of the Interior of Taiwan. We obtained the city/county-specific relative risks (RRs) for all-cause (non-accidental), cardiovascular, and respiratory disease mortality for each degree of daily average temperature during 1995–2008 from an epidemiology study in Taiwan (Lin et al., 2019).

2.2. Statistical model for short-term prediction of annual extremely hot days

We developed a state-space model for the number of extremely hot days with daily mean temperatures exceeding T°C, 26 ≤ T ≤ 32 during June–September. A state-space model allows parameter estimation from a single observed time series for the underlying deterministic process, observation error, and process error (Bolker, 2008). The temperature limits of 26 °C and 32 °C were determined based on the RRs of mortality compared to 25 °C of an epidemiological study in Taiwan (Lin et al., 2019) and historical temperature records. A separate model was established for each of the 24 meteorological stations across Taiwan. For simplicity, we skipped the subscript i for the i-th station in the following. Let the number of days with daily mean temperature exceeding T of year k be $Y_{T,k}$. A statistical prediction model for $Y_{T,k}$ based on the estimated trend $\mu_{T,k}$ due to climate change and the lagged influence of Niño 3.4 can be written as

$$Y_{T,k} = \mu_{T,k} + f(Nino3.4, l; T, k) + X_{T,k} + \nu_{T,k} \quad (1)$$

where f($Nino3.4, l; T, k$) is a mean-adjusted nonlinear function relating the Niño 3.4 index of lagged month l to $Y_{T,k}$, $X_{T,k}$ is a stationary time series with variation that is not explained by the first two factors, and $\nu_{T,k}$ is the observational error, which is assumed to be normally distributed with mean 0 and variance σ_{obs}^2. Following Lorenz's work on chaotic theory (Lorenz, 1963), probabilistic approaches for climate-change projections have become dominating in the weather and climate forecasting science, as described by Slingo and Palmer (2011). Here, we assumed that the uncertainty in climate change trend $\mu_{T,k}$ can be described by a nonlinear time-dependent function $g_T(k)$ plus a random noise $e_{T,k}^*$. Following Taylor's polynomial approximation at the 1st degree (Weisstein, 2004), after some algebra, we have

$$\begin{aligned}\mu_{T,k} &= g_T(k) + e_{T,k}^* \cong g_T(k-1) + g_T'(k-1) * [k-(k-1)] \\ &\quad + e_{T,k}^* \cong 2\mu_{T,k-1} - \mu_{T,k-2} + e_{T,k}\end{aligned} \quad (2)$$

where $e_{T,k}$ is the process error, which is assumed to be normally distributed with mean 0 and variance σ_{proc}^2. We applied a locally weighted scatter plot smoothing (LOESS) regression curve to estimate f($Nino3.4, l; T, k$). Because the time series of the trend-removed residuals of $Y_{T,k}$ may be time-dependent, we assumed that the variation $X_{T,k}$ follows an autoregressive moving average (ARMA) model, i.e.

$$X_{T,k} = \sum_{r=1}^{p} \varphi_r X_{k-r} + \sum_{s=1}^{q} \zeta_s \varepsilon_{k-s} + \varepsilon_k \quad (3)$$

where ε_k are uncorrelated random quantities with mean 0 and variance σ^2. The Niño 3.4 index of the lagged month l corresponding to the index in July of next year was used for the estimation of $f(Nino3.4, l; T, k)$. Based on the model using a calibration period of 1951–2014, we assessed the performance of the model over a validation period of 2015–2017.

To differentiate the process error from the observation error of the state-space model (Eqs. (1)–(2)), we adopted a Bayesian framework using Markov-chain Monte Carlo (MCMC) simulations to estimate the model parameters (Bolker, 2008). We performed the MCMC simulations using OpenBUGS version 3.2–3.1 (MRC Biostatistics Unit, Cambridge, UK), and conducted nonliner lagged analyses using a free software Distributed Lag Non-linear Models (DLNM) version 2.2.6. We employed the R-package version 3.3.2 to estimate the LOESS regression curve. The OpenBUGS simulation program for the predictions is given in the Supplementary Materials (SM).

2.3. Short-term projection of heat-related mortality due to climate change

We assessed the heat-attributable mortality due to climate change using the "counterfactural method" of CRA (Patz et al., 2008). We compared the AM resulting from the difference in distribution of the number of extremely hot days between the predicted year and the reference period 2001–2010. Specifically, we calculated AM following the equation.

$$AM = Pop \times M \times PAF \tag{4}$$

where Pop is the population size, M is the mortality rate, and PAF is the population attributable fraction (PAF). We estimated PAF using the equation

$$\mathrm{PAF} = 1 - \frac{\int_U^{U^*} RR(x)P'(x)dx}{\int_U^{U^*} RR(x)P(x)dx} \tag{5}$$

where $RR(x)$ is the RR at temperature x, $P(x)$ and $P'(x)$ are the probability density functions of the temperature x for the predicted year and the reference period, respectively, U is the temperature threshold, and U^* is the upper limit.

3. Results

3.1. Predictions

We analyzed the meteorological records during 1951–2017 for the climate change trend at each of the 24 meteorological stations across Taiwan. For conciseness, we show four stations located in the cities/counties of Taipei, Taichung, Kaohsiung, and Hualien to represent the analysis results over the northern, central, southern, and eastern parts of Taiwan, respectively. Fig. 1 shows the number of days exceeding the 90% and 95% temperature percentiles of the baseline period 1961–1990 at each station. There was an approximately exponentially increasing trend in extremely high temperature days at all four stations.

We assessed the influence of ENSO on the number of days with extreme heat in Taiwan. Fig. 2 shows the association between the lagged Niño 3.4 index and days with extremely high temperature in June–September during 1951–2017 at the four stations. The contour graphs of the RR of days with daily average temperatures exceeding the 95% percentile during 1951–1990 (Fig. 2a) show a maximum around 6–8 month lags and a minimum around 0 or 12 month lags when there was a strong El Niño or La Niña phenomenon. This association was similar for the four stations assessed. A lag of 8 months was determined based on the administrative purpose of prediction in the previous year. That is, we used the Niño 3.4 index of November for the prediction of hot days in June–September of the next year. Fig. 2 (b) shows the association between the days of extremely high temperature and the Niño 3.4 index with a lag of 8 months during 1951–2017. For all four stations investigated, the days of extremely hot temperatures greater than the 95th or 90th percentile increased with the Niño 3.4 index, which had a small peak at Niño 3.4 around 0.

To estimate the climate change trend excluding the impact of ENSO, we calculated the number of days after adjusting for the lagged effect of Niño 3.4, i.e., $y_{T,k}^* = y_{T,k} - f(Nino3.4, l; T, k)$. Fig. S1 shows the annual $y_{T,k}^*$ for the four stations– in Taipei, Taichung, Kaohsiung, and Hualien from 1951 to 2017 with daily mean temperatures exceeding 30 °C together with the LOESS curve for the trend estimate (SM). Taipei and Kaohsiung had an exponentially increasing trend of $y_{T,k}^*$ since 2000, whereas the trends for Taichung and Hualien were relatively minor. The plots of the trends for the days exceeding other mean temperatures were similar.

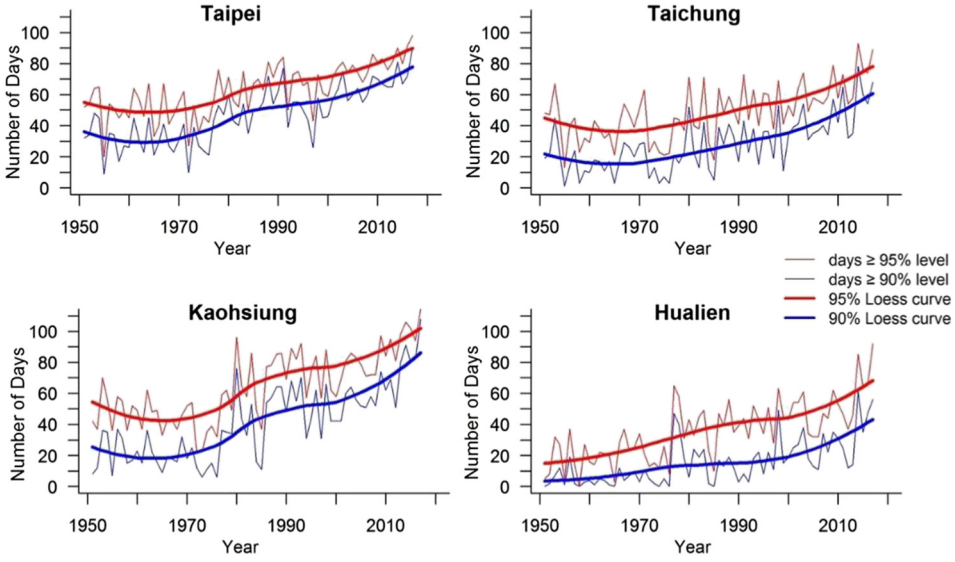

Fig. 1. The number of days exceeding the 95th (red) and 90th (blue) temperature percentiles between June and September of the baseline period 1951–1990 in Taipei (north), Taichung (central), Kaohsiung (south), and Hualien (east). The lines corresponding to the 95th (red) and 90th (blue) percentiles were separate locally weighted scatter plot smoothing (LOESS) regression curves.

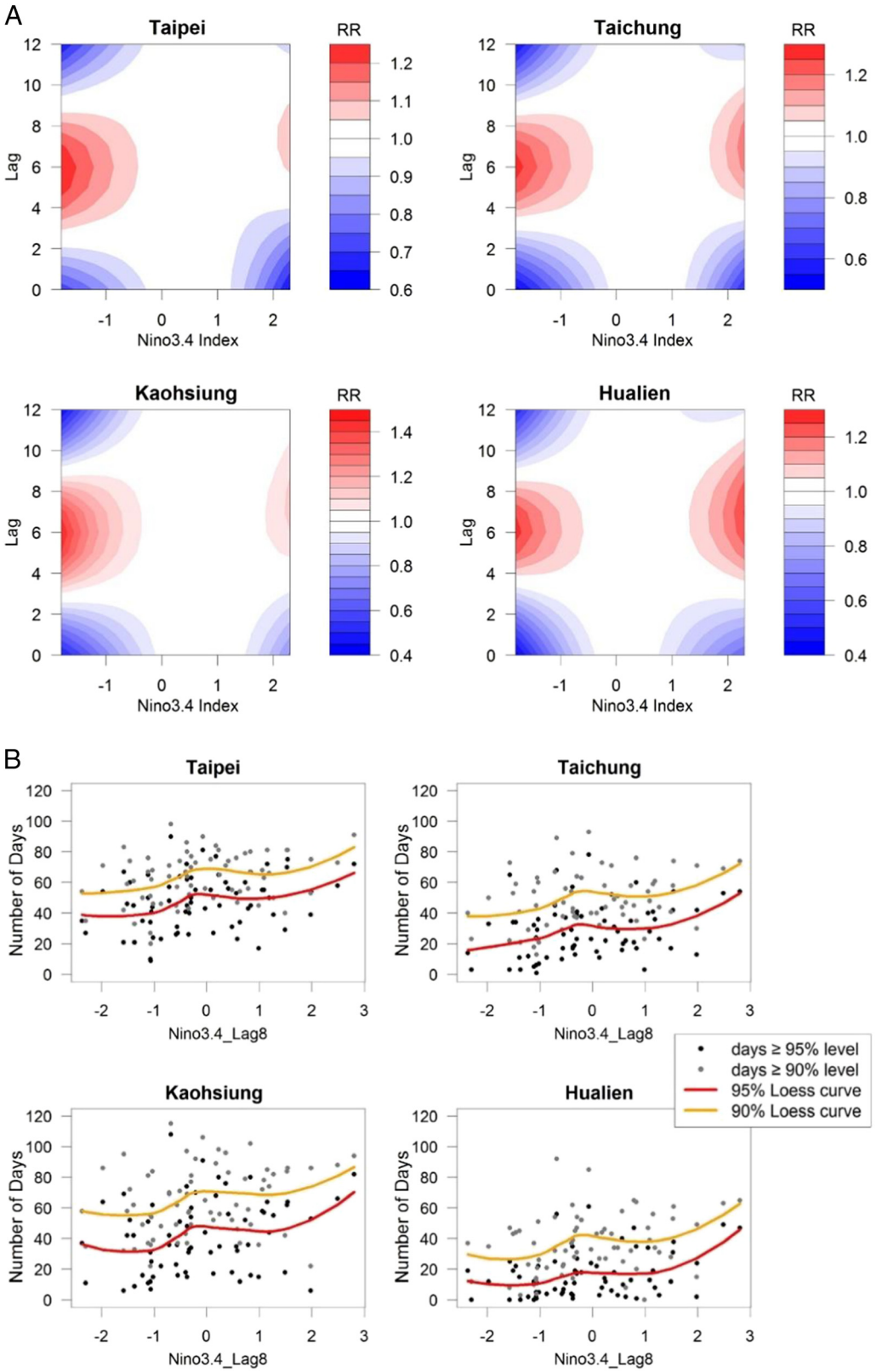

Fig. 2. Associations between lagged Niño 3.4 index and days with average temperature extremes in June–September during 1951–2017: (a) the contour graphs of the relative risk of days exceeding the 95th percentile versus the Niño 3.4 index at different lags; (b) days exceeding the upper 95th (dark circle) and 90th (light circle) percentile separately versus the Niño 3.4 index at an 8 month lags. The lines corresponding to the 95th (red) and 90th (orange) percentiles of the baseline period 1951–1990 were separate locally weighted scatter plot smoothing (LOESS) regression curves.

Similar to the estimation of the lagged effect of Niño 3.4 on the number of extremely hot days, we applied a LOESS regression curve for the climate change trend estimates $\hat{\mu}_{T,k-1}, \hat{\mu}_{T,k-2}$ up to year k − 1. A prediction for the climate change trend of year k is then $2\hat{\mu}_{T,k-1} - \hat{\mu}_{T,k-2}$ following Eq. (2). For the stationary time series variation $X_{T,k}$ of Eq. (1), an autoregressive model of order 2 (AR(2)) was determined.

Fig. S2 shows the partial autocorrelation function (PACF) plots of the model residuals for the four stations, which showed satisfactory results from model fitting (SM). To verify the normal distributional assumption of the model residual $\nu_{T,k}$ given in Eq. (1), we plotted the Q-Q plot for the quantiles of the residuals $\nu_{T,k}$ versus the quantiles of the standard normal distribution. Fig. S3 displays the Q-Q plots of the 4 representative cities/counties (Taipei, Taichung, Kaohsiung, Hualien) for temperatures 26 °C–30 °C. The plots showed that for all the 4 cities/counties, the normal distributional assumption approximately held except for 30 °C with heavy tails for the residuals. Alternative extreme value distributional assumption might be needed for daily mean temperature exceeding 30 °C. However, because the corresponding number of days is very limited, the prediction outcomes should not be affected much.

Following the same procedure, we established a prediction model for each of the 24 stations across Taiwan. Because mountainous areas such as the Central Mountain Range cover approximately 70% of the island, we divided the main island of Taiwan into seven ENSO-impacted zones based on the historical temperature record of each station and the geographical homogeneity of neighboring counties. A single ENSO effect function $f(Nino3.4, l; T, k)$ was shared for stations falling within the same zone. Fig. 3 shows the division of the seven zones across Taiwan. To demonstrate the heterogeneity among different zones, Fig. S4 shows the number of days with extreme heat in the seven zones during 2015–2017 (SM). The number of hot days in Zone 2 (northern Taiwan including Taipei) and Zone 5 (southern Taiwan including Kaohsiung) were substantially higher than those of other zones, whereas Zone 7 (eastern Taiwan including Hualien) had relatively fewer days.

To assess the performance of the established model, Fig. 4 shows the errors (3-year average) between the predictions and the observed hot days with daily mean temperatures exceeding 26 °C to 32 °C in 2015–2017 for each of the 24 stations. The results showed that approximately 65% of the cells had an error within 2 days and 84% within 4 days. Only 3 out of 135 (≅2%) cells had a prediction error >10 days. Thus, the predictions were highly precise.

Using the Niño 3.4 index from November 2017, together with the estimated trend, we predicted the number of extremely hot days of the 24 stations in 2018. Fig. 5 shows the prediction map of days exceeding 29 °C, 30 °C, and 31 °C across Taiwan together with the predicted number of days at the 24 stations. The predictions for the sites other than the 24 stations were obtained using the inverse distance weighting technique. For almost all the main residential areas in western Taiwan, the number of days exceeding 29 °C was >50, with the highest prediction of 82 days in Kaohsiung followed by 75 days in Taipei. For daily mean temperatures exceeding 30 °C (31 °C), Taipei had the highest prediction at 53 (23) days followed by 42 (9) days in Kaohsiung. In contrast, the predicted numbers of hot days in Hualien of eastern Taiwan was much smaller, with the

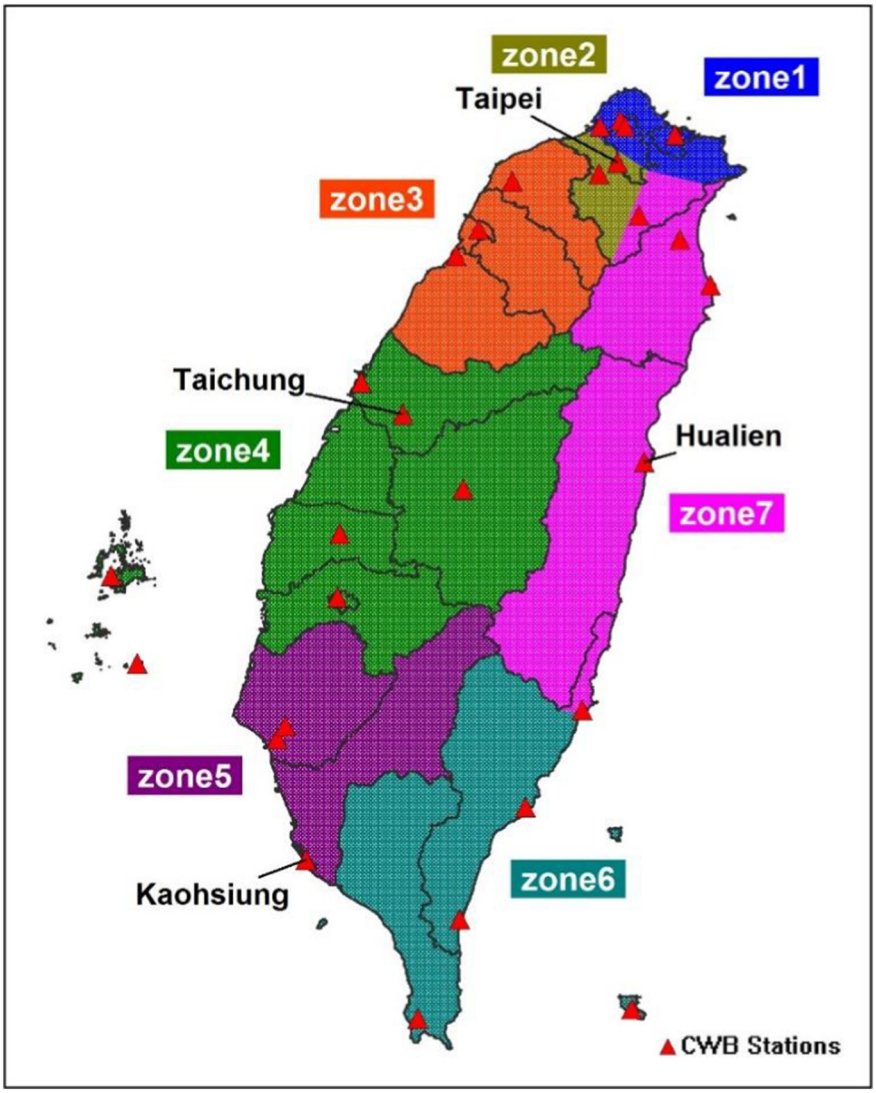

Fig. 3. Division of the administrative areas in Taiwan into 7 zones that are affected by the Niño 3.4 index.

Station / Year / Temperature	Tonghou	Xinwu	Zhunan	Huwei	Banqiao	Tamsui	**Taipei**	Keelung	**Hualien**	Suao	Yilan	Dongjidao	Penghu	Tainan	Yongkang	**Kaohsiung**	Chiayi	**Taichung**	Dawu	Hsinchu	Hengchun	Chengkung	Taitung	Wuqi
≥ 26 °C	4	0	0	3	2	4	1	0	-1	1	2	0	-1	2	-2	1	1	2	-1	1	0	0	-1	1
≥ 27 °C	2	0	-1	7	1	4	4	1	0	3	2	0	0	3	-1	1	5	3	-1	5	-2	3	1	4
≥ 28 °C	3	-3	1	13	0	5	3	1	-1	5	5	-2	2	3	-2	-1	4	1	1	7	-2	5	-1	5
≥ 29 °C	5	-3	0	11	4	6	3	2	-1	5	2	1	-3	4	-2	-2	1	2	-1	7	-6	8	0	3
≥ 30 °C	NA	1	1	9	11	2	4	0	-1	0	0	0	1	0	-3	-8	-3	1	4	2	-8	2	-2	1
≥ 31 °C	NA	1	-1	2	2	0	-1	-2	NA	0	0	NA	0	0	-1	-3	-1	1	0	-2	-1	NA	2	NA
≥ 32 °C	NA	NA	NA	NA	0	1	-2	-1	NA	NA	NA	NA	NA	NA	NA	0	NA	NA	0	0	NA	NA	NA	NA

Fig. 4. Prediction errors of extremely hot days with daily mean temperatures exceeding 26 °C to 32 °C in June–September for each of the 24 meteorological stations across Taiwan during 2015–2017 (3-year average).

numbers of days exceeding 29 °C, 30 °C, and 31 °C being 44, 8, and 0 days, respectively.

As a comparison, we have also predicted the number of days with maximum temperature between 29 °C and 38 °C using the model given in Eq. (1). The contour plots of the association between lagged Niño 3.4 index and number of days exceeding the 95th and 90th daily maximum temperature are given in Fig. S5 (SM), respectively. The results showed that the associations with the lagged Nino3.4 index were very similar to those with daily mean temperature. Prediction errors also showed that approximately 93% of the cells were within −5 to 7 days for the 3 years average during 2015–2017 (Fig. S6, SM).

3.2. Projections of attributable mortalities due to extremely hot days relative to 2000–2010

Based on the above outcomes, we projected the heat-related AMs of all-causes, circulatory diseases, and respiratory diseases relative to the reference period 2001–2010 for each of the 19 cities/counties in 2018 in Taiwan. For cities/counties with more than one meteorological station, we used the average predicted number of days at all stations within the same city/county. In practice, we approximated the integral in Eq. (5) by

$$\int_T^m RR(x)P(x)dx \cong \sum_{l=27}^{32} RR(l)[P(Tmpt \geq l-1) - P(Tmpt \geq l)]$$

$$\cong \sum_{l=27}^{32} RR(l)\left(\hat{y}_{l-1,k} - \hat{y}_{l,k}\right),$$

where the abbreviation Tmpt is daily mean temperature. Similarly, we approximated the integral $\int_T^m RR(x)P'(x)dx$ in the same way. We used the population size and mortality data at the end of 2016 for the calculation of AMs. The projected PAFs and AMs were rounded to 0 if the results were negative. Fig. 6 shows the projected PAF, AM, and AM per 100 km^2 for each city/county in 2018. The projected PAFs showed that northern Taiwan had more severe impact of heat-related mortality due to climate change compared to other areas, with PAF ranged from 0.015 to 0.333 (Fig. 6(a)). As a result, the Taipei metropolitan area (Taipei and New Taipei City), the densest populated area in Taiwan, had the highest heat-related AMs, followed by Taichung, which has the third largest population (Fig. 6(b)). Counties in eastern Taiwan would have the least heat-related AMs due to less climate change impact and low population density. The predicted numbers of days in Fig. 5 are the means of the MCMC simulated outcomes. The estimated RRs of temperature-related mortalities at each city/county contributed an additional source of uncertainty. As a result, the projected outcomes might have a wide confidence interval. Table 1 summarizes the mean projected AMs of Taipei/New Taipei, Taichung, Kaohsiung, and Hualien in 2018. For the first 3 cities/counties with population sizes of 2.8 to 6.7 million, the 95% CIs of the projected all-cause AMs ranged from 0 to 4785, whereas for Hualien, the mountainous area with the lowest population density, the range was 61 to 186.

4. Discussion

We have shown in this study that in addition to the influence of ENSO, climate change has an imminent impact on the number of days

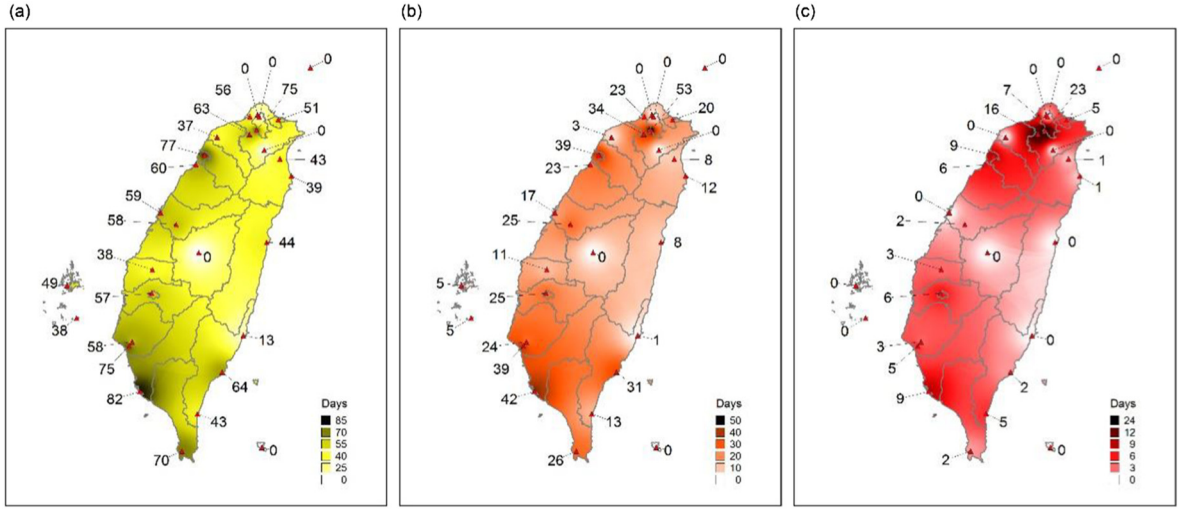

Fig. 5. Predicted number of days with daily mean temperature in June–September exceeding (a) 29 °C, (b) 30 °C, and (c) 31 °C in 2018.

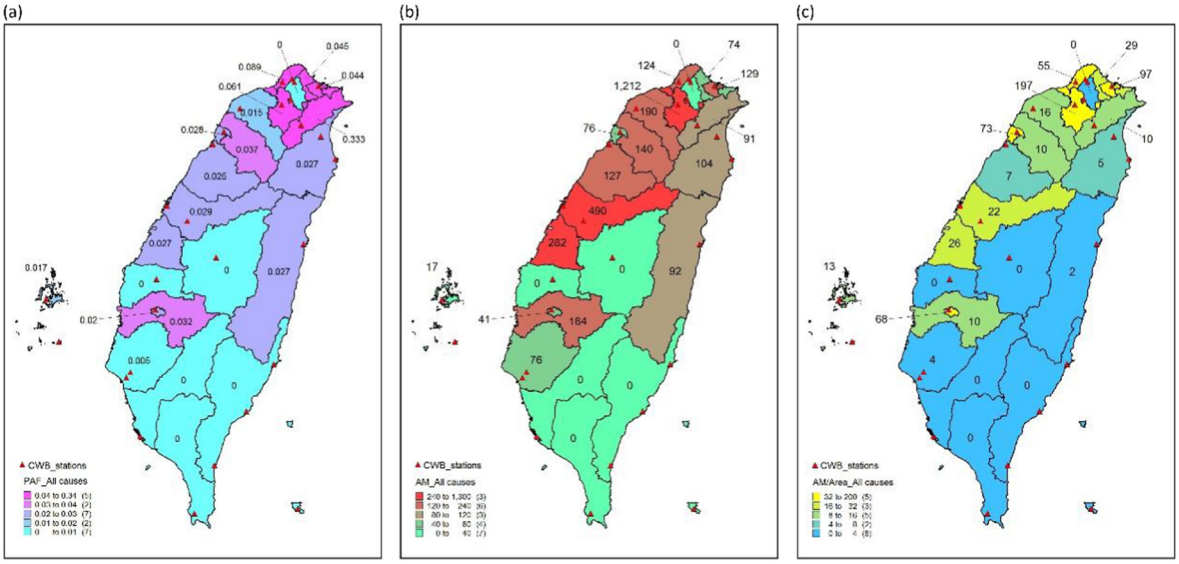

Fig. 6. Projected attributable population fractions (PAFs) and attributable mortalities (AMs) (a) PAFs, (b) AMs, and (c) AMs per 100 km^2 relative to the reference period 2001–2010 for each city/county in 2018.

with extremely hot temperatures in Taiwan. As a result, heat-attributable mortality is expected to increase compared to that in the last decade (2001−2010). Areas with high population density such as New Taipei City and Taichung are most likely to experience more severe impacts than other cities/counties, whereas mountainous areas such as eastern Taiwan are less affected. The results can serve as guidance for medical resource allocation to prevent heat-related mortality, and risk maps can be used for health policy administration purposes (e.g., Fig. 6).

We conducted a short-term prediction of extremely hot days from Eq. (1) primarily based on two influential factors: estimated climate change trend and lagged effect of Niño 3.4 index. The results showed that for most areas in Taiwan, the number of days with extreme heat continues to increase in 2018. This is mainly due to the estimated upward climate change trend in the number of days with extreme heat, as shown in Fig. 1 and Fig. S1, after adjusting for the lagged effect of Niño 3.4 (SM). We estimated the climate change trend on a yearly basis together with the process error, as shown in Eq. (2). This approach has the advantage of flexibility in that adjustments can be made year by year rather than a linear model estimate for several decades (Guttorp and Xu, 2011; Zhang et al., 2018).

Our findings of lagged association between Niño 3.4 index and hot days in summer (Fig. 2) are consistent with climatology studies in China and Indochina peninsula, which is characterized by anomalous rising motion over the tropical central Pacific and Indian Oceans (Lin et al., 2018; Luo and Lau, 2018; Wang et al., 2017). However, unlike these studies that stress on the underlying mechanisms and spatiotemporal associations among various atmospheric factors, our primary goal was on statistical prediction using the lagged association. Furthermore, our proposed model is able to capture the nonlinear associations both with climate change trend and lagged Niño 3.4 index. Other existing statistical models, however, only involves linear terms that might not hold under certain circumstances (Qian et al., 2015; Zhang et al., 2018).

In contrast with the climate model simulation results from the IPCC based on various RCP scenarios (Guo et al., 2017), statistical time-series models using observed historical data provide short-term predictions with much less uncertainty. As shown in Fig. 4, the 3-year average prediction errors for all 24 stations had a very high precision compared to the observed number of days of the station within the period, with 84% of the cells falling within 4 days. Therefore, the presented statistical model can be used reliably for the short-term prediction of summer days with extreme heat as an early warning tool to mitigate heat-related health hazards. We presented the predicted outcomes (Fig. 5) and the resultant projected PAFs and AMs (Fig. 6) for 2018. While predictions for the next few years are available, the spring predictability barrier of ENSO (Fang and Mu, 2018) may affect their accuracy, which is conventionally limited to 6 months into the future. Ludescher et al. (2014) propose a network analysis-based approach that allows projection of an El Niño event up to one year ahead. Furthermore, Fig. 2 (b) shows that the lagged Niño 3.4 index had a major impact on the number of days with extreme heat only when there was a strong El Niño. Therefore, one may still rely on short-term predictions using the presented model with high reliability when there is slight variation in Niño 3.4 index prediction.

We applied Bayesian MCMC simulations for the estimation of model parameters as well as the predictions. Because of the sequentially nested structure of the proposed state-space model, a Bayesian approach using MCMC simulations provides a natural computational tool for the implementation of the dynamic model (Bolker, 2008). We employed a CRA approach to the health impact assessment of heat-related mortalities due to climate change (Patz et al., 2008). While this

Table 1
Mean projected heat-attributable all-cause mortalities for Taipei/New Taipei, Taichung, Kaohsiung, and Hualien in 2018 (reference period 2000–2010). The numbers in the parentheses are the corresponding 95% CI.

City/county	Area (km^2)	Population	Heat-attributable mortalities		
			PAF	AM	AM/100 km^2
Taipei/New Taipei	2324.4	6,674,912	0.089 (0.06–0.127)	1501 (82–4785)	290 (31–915)
Taichung	2214.9	2,767,239	0.029 (0–0.069)	490 (0–1166)	22 (0–53)
Kaohsiung	2951.9	2,779,371	0 (0–0.002)	0 (0–43)	0 (0–3)
Hualien	4628.6	330,911	0.027 (0.018–0.055)	92 (61–186)	2 (1–4)

AM, attributable mortality; PAF, population attributable fraction.

approach is often used to assess related health impacts for several decades into the future, here, we assessed the impact for a relatively short period of only a few years. As shown in Fig. 1, the number of days with extreme heat has been monotonically increasing for the last few decades at all four representative stations in Taiwan. Therefore, even for a very short period of time, an upward trend is expected. As a result, the projected AMs could reach into the thousands for several cities/counties relative to 2001–2010, though there is a great degree of uncertainty (Table 1).

Studies have found that the threshold of temperature-related mortality varies across different countries (Gasparrini et al., 2015; Guo et al., 2014). Although Taiwan is a relatively small island of 35,873 km^2, the same phenomenon was also found (Lin et al., 2012). This might be attributable to different age distributions, socioeconomic status, and geophysical heterogeneity. We used city/county- and temperature-specific RRs to estimate the projected AMs across Taiwan. Because local residents are more frequently accustomed to increasing heat in the summer season, the heat-related AMs might be smaller than projected. Adaptations for climate change may be accomplished through adjustments for physiological acclimatization, behavior patterns such as avoiding outdoor activities during extreme heat, or the use of air conditioning (Chung et al., 2009).

There are some limitations of the current study. First, we assumed that the state-space model error is normally distributed. The Q-Q plots given in Fig. S3 (SM) showed that this distributional assumption held approximately. However, for temperature exceeding 30 °C, alternative distributional assumptions such as extreme-value distributions might be more appropriate. Second, the grouping of the Taiwan island into 7 NOSO-impacted zones was somewhat subjective. One may reclassify stations near the borders into different zones. We checked the records of each station individually to reconfirm the grouping and homogeneity within the same zone. The result seemed appropriate and was also supported by the heterogeneity among different zones (Fig. S4, SM). Third, the daily average heat index instead of the ambient temperature may be a more suitable temperature index for estimating projected AMs because of the subtropical climate with yearlong high humidity in Taiwan (Sung et al., 2013). Further studies along these lines are necessary.

5. Conclusions

We have developed a statistical state-space model considering the impacts of climate change and ENSO for the short-term prediction of summer days with extreme heat. The validation study showed that the model performed well, with 84% of the 3-year average prediction errors within 4 days compared to the historical data (2015–2017) across Taiwan. Based on the presented model, the Taipei metropolitan area had the largest projected AMs in 2018, followed by Taichung, the most populated areas in northern and central Taiwan, respectively. The impacts for southern and eastern Taiwan were relatively mild. The prediction model and the projected outcomes may serve as a tool and guidance for developing effective health policy in the face of imminent impacts of climate change on public health.

Acknowledgements

This research was supported by the grants MOST 105-2118-M-400-003 and MOST 106-2118-M-400-004 from the Ministry of Science and Technology of Taiwan and NHRI-107-EMSP03 from the Ministry of Health and Welfare. The authors acknowledge support from the National Applied Research Laboratories of the Taiwan Typhoon and Flood Research Institute to provide the Data Bank for Atmospheric & Hydrologic Research.

Appendix A. Supplementary data

Supplementary data to this article can be found online at https://doi.org/10.1016/j.scitotenv.2019.01.168.

References

Bolker, B., 2008. Ecological models and data in R. Chapter 11. Dynamic Models. Princeton University Press, Princeton, New Jersey, pp. 445–470.
Cannon, A.J., 2015. Revisiting the nonlinear relationship between ENSO and winter extreme station precipitation in North America. Int. J. Climatol. 35, 4001–4014.
Chen, S.-T., Yang, T.-C., Kuo, C.-M., Kuo, C.-H., Yu, P.-S., 2013. Probabilistic drought forecasting in southern Taiwan using El Niño-Southern Oscillation Index. Terr. Atmos. Ocean. Sci. 24 (5), 911–924.
Chung, J.-Y., Honda, Y., Hong, Y.-C., Pan, X.-C., Guo, Y.-L., Kim, H., 2009. Ambient temperature and mortality: an international study in four capital cities of East Asia. Sci. Total Environ. 408, 390–396.
Fang, X.-H., Mu, M., 2018. Both air-sea components are crucial for El Niño forecast from boreal spring. Sci. Rep. 8, 10501.
Gasparrini, A., Guo, Y., Hashizume, M., Lavigne, E., Zanobetti, A., Schwartz, J., et al., 2015. Mortality risk attributable to high and low ambient temperature: a multicountry observational study. Lancet 386, 369–375.
Guo, Y., Gasparrini, A., Armstrong, B., Li, S., Tawatsupa, B., Lavigne, E., et al., 2014. Global variation in the effects of ambient temperature on mortality: a systematic evaluation. Epidemiology 25 (6), 781–789.
Guo, X., Huang, J., Luo, Y., Zhao, Z., Xu, Y., 2017. Projection of heat waves over China for eight different global warming targets using 12 CMIP5 models. Theor. Appl. Climatol. 128, 507–522.
Guttorp, P., Xu, J., 2011. Climate change, trends in extremes, and model assessment for a long temperature time series from Sweden. Environmetrics 22 (3), 456–463.
Honda, Y., Kondo, M., McGregor, G., Kim, H., Guo, Y.-L., Hijioka, Y., et al., 2014. Heat-related mortality risk model for climate change impact projection. Environ. Health Prev. Med. 19, 56–63.
Kuo, C.-C., Gan, T.Y., Yu, P.-S., 2010. Wavelet analysis on the variability, teleconnectivity, and predictability of the seasonal rainfall of Taiwan. Mon. Weather Rev. 138, 162–175.
Larkin, N.K., Harrison, D.E., 2005. Global seasonal temperature and precipitation anomalies during El Niño autumn and winter. Geophys. Res. Lett. 32, L16705.
Lee, J.Y., Kim, H., 2016. Projection of future temperature-related mortality due to climate and demographic changes. Environ. Int. 94, 489–494.
Leung, M.Y.T., Zhou, W., 2016. Direct and indirect ENSO modulation of winter temperature over the Asian–Pacific–American region. Sci. Rep. 6, 36356.
Lin, Y.-K., Chang, C.-K., Li, M.-H., Wu, Y.-C., Wang, Y.-C., 2012. High-temperature indices associated with mortality and outpatient visits: characterizing the association with elevated temperature. Sci. Total Environ. 427–428, 41–49.
Lin, L., Chen, C., Luo, M., 2018. Impacts of El Niño-Southern Oscillation on heat waves in the Indochina peninsula. Atmos. Sci. Lett. 19, e856.
Lin, Y.-K., Maharani, A.T., Chang, F.-T., Wang, Y.-C., 2019. Mortality and morbidity associated with ambient temperatures in Taiwan. Sci. Total Environ. 651, 210–217.
Lorenz, E.N., 1963. Deterministic nonperiodic flow. J. Atmos. Sci. 20, 130–141.
Ludescher, J., Gozolchina, A., Bogachev, M.I., Bunde, A., Havlin, S., Schellnhuber, J., 2014. Very early warning of next El Niño. PNAS 111 (6), 2064–2066.
Luo, M., Lau, N.-C., 2018. Amplifying effect of ENSO on heat waves in China. Clim. Dyn. https://doi.org/10.1007/s00382-018-4322-0.
Nitschke, M., Tucker, G.R., Hansen, A., Williams, S., Zhang, Y., Bi, P., 2011. Impact of two recent extreme heat episodes on morbidity and mortality in Adelaide, South Australia: a case-series analysis. Environ. Health 10 (1), 42.
NOAA, January 2017. National Centers for Environmental Information, State of the Climate: Global Climate Report for Annual 2016. Available at:. http://www.ncdc.noaa.gov/sotc/global/201613, Accessed date: 14 April 2017.
Patz, J., Campbell-Lendrum, D., Gibbs, H., Woodruff, R., 2008. Health impact assessment of global climate change: expanding on comparative risk assessment approaches for policy making. Annu. Rev. Public Health 29, 27–39.
Peng, D., Wang, X., Zhao, C., Wu, X., Jiang, F., Chen, P., 2014. Characterizing air temperature changes in the Tarim Basin over 1960–2012. PLoS One 9 (11), e112231.
Perkins, S.E., 2015. A review on the scientific understanding of heatwaves— their measurement, driving mechanisms, and changes at the global scale. Atmos. Res. 164, 242–267.
Qian, C., Zhou, W., Fong, S.K., Leong, K.C., 2015. Two approaches for statistical prediction of non-Gaussian climate extremes: a case study of Macao hot extremes during 1912–2012. J. Clim. 28 (2), 623–636.
Ratnam, J.V., Behera, S.K., Annamalai, H., Ratna, S.B., Rajeevan, M., Yamagata, T., 2016. ENSO's far reaching connection to Indian cold waves. Sci. Rep. 6, 37657.
Rohini, P., Rajeevan, M., Srivastava, A.K., 2016. On the variability and increasing trends of heat waves over India. Sci. Rep. 6, 26153.
Slingo, J., Palmer, T., 2011. Uncertainty in weather and climate prediction. Phil. Trans. R. Soc. A 369, 4751–4767.
Stephenson, D.B., Collins, M., Rougier, J.C., Chandler, R.E., 2012. Statistical problems in the probabilistic prediction of climate change. Environmetrics 23, 364–372.
Sung, T.-I., Wu, P.-C., Lung, S.-C., Lin, C.-Y., Chen, M.-J., Su, H.-J., 2013. Relationship between heat index and mortality of 6 major cities in Taiwan. Sci. Total Environ. 442, 275–281.
Vandentorren, S., Bretin, P., Zeghnoun, A., Mandereau-Bruno, L., Croisier, A., Cochet, C., et al., 2006. Heat-related mortality– August 2003 heat wave in France: risk factors for death of elderly people living at home. Eur. J. Pub. Health 16 (6), 583–591.
Wang, P., Tang, J., Sun, X., Wang, S., Wu, J., Dong, X., et al., 2017. Heat waves in China: definitions, leading patterns, and connections to large-scale atmospheric circulation and SSTs. J. Geophys. Res. Atmos. 122, 10679–10699.
Weisstein, E.W., 2004. Taylor Series. MathWorld–A Wolfram Web Resource. http://mathworld.wolframe.com/TaylorSeries.html.
Zhang, J., Yang, Z., Wu, L., 2018. Skillful prediction of hot temperature extremes over the source region of ancient Silk Road. Sci. Rep. 8, 6677.
Zuo, J., Pullen, S., Palmer, J., Bennetts, H., Chileshe, N., Ma, T., 2015. Impacts of heat waves and corresponding measures: a review. J. Clean. Prod. 92, 1–12.